BJP British Journal of Pharmacology | BPS BRITISH PHARMACOLOGICAL SOCIETY

Differential sensitivity of TREK-1, TREK-2 and TRAAK background potassium channels to the polycationic dye ruthenium red

Journal:	*British Journal of Pharmacology*
Manuscript ID:	2014-BJP-0838-RP.R1
Manuscript Type:	Research Paper
Date Submitted by the Author:	15-Oct-2014
Complete List of Authors:	Braun, Gabriella; Semmelweis University, Department of Physiology Lengyel, Miklós; Semmelweis University, Department of Physiology Enyedi, Péter; Semmelweis University, Department of Physiology Czirják, Gábor; Semmelweis University, Department of Physiology
Major area of pharmacology:	Pain
Cross-cutting area:	Electrophysiology
Additional area(s):	Ion channels

Differential sensitivity of TREK-1, TREK-2 and TRAAK background potassium channels to the polycationic dye ruthenium red

Abbreviated title: Sensitivity of K2P channels to ruthenium red

G Braun, M Lengyel, P Enyedi and G Czirják

Department of Physiology, Semmelweis University, Budapest, Hungary

Corresponding author: Gábor Czirják, M.D., Ph.D., Department of Physiology, Semmelweis University, P. O. Box 259, H-1444 Budapest, Hungary, Phone: (36-1-) 459-1500/60433, Fax: (36-1-) 266-7480, e-mail: czirjak.gabor@med.semmelweis-univ.hu

SUMMARY

BACKGROUND AND PURPOSE: Pharmacological separation of the background potassium currents of closely related K2P channels is a challenging problem. We previously demonstrated that ruthenium red (RR) inhibits TASK-3 (K2P9) but not TASK-1 (K2P3) channel. RR has been extensively used to distinguish between TASK currents in native cells. In the present study, we systematically investigate the RR sensitivity of a more comprehensive set of K2P channels.

EXPERIMENTAL APPROACH: K^+ currents were measured by two-electrode voltage clamp in *Xenopus* oocytes and by whole-cell patch clamp in mouse dorsal root ganglion (DRG) neurons.

KEY RESULTS: Ruthenium red differentiates between two closely related members of the TREK subfamily. TREK-2 (K2P10) proved to be highly sensitive to RR (IC_{50}=0.2 μM), whereas TREK-1 (K2P2) was not affected by the compound. We identified aspartate 135 (D135) as the target of the inhibitor in mouse TREK-2c. D135 lines the wall of the extracellular ion pathway (EIP), a tunnel structure through the extracellular cap characteristic for K2P channels. TREK-1 contains isoleucine in the corresponding position. The mutation of this isoleucine (I110D) rendered TREK-1 sensitive to RR. The third member of the TREK subfamily, TRAAK (K2P4) is more potently inhibited by ruthenium violet, a contaminant in some RR preparations, than by RR. DRG neurons predominantly express TREK-2 and RR-resistant TREK-1 and TRESK (K2P18) background K^+ channels. We detected the RR-sensitive leak K^+ current component in DRG neurons.

CONCLUSIONS AND IMPLICATIONS: We propose that RR may be useful for distinguishing TREK-2 from TREK-1 and other RR-resistant K2P channels in native cells.

KEYWORDS: two-pore domain, potassium channel, ruthenium red, TREK2, KCNK2, KCNK10, TALK-1, TASK-2, THIK-1

ABREVIATIONS

DRG dorsal root ganglion

K2P two-pore-domain K^+ (channel)

RR ruthenium red

RV ruthenium violet

TALK TWIK-related alkaline-activated K^+ channel

TASK TWIK-related acid-sensitive K^+ channel

THIK TWIK-related halothane-inhibited K^+ channel

TRAAK TWIK-related arachidonic acid-activated K^+ channel

TREK TWIK-related K^+ channel

TRESK TWIK-related spinal cord K^+ channel

TWIK tandem of pore domains in a weakly inwardly rectifying K^+ channel

INTRODUCTION

Different members of the two-pore domain (K2P) K^+ channel family show characteristic expression patterns, they are regulated by extraordinarily diverse mechanisms, and contribute to a great variety of physiological processes (Enyedi and Czirják, 2010). These channels give rise to similar macroscopic background (leak) potassium currents, and thus it is a challenge to distinguish them in whole-cell measurements. Identification of individual K2P channel types is also of importance because the different members of the family may prove to be therapeutic targets in distinct pathophysiological states (Mathie and Veale, 2007; Bittner *et al.*, 2010). Pharmacological properties of K2P channels have been extensively investigated; however, the background K^+ currents were typically affected by relatively nonspecific compounds (Lotshaw, 2007). It appears to be difficult to identify highly selective inhibitors of K2P channels, perhaps because of the distinctive structural element, the extracellular cap, which covers the entrance of the ion conducting pore, and restricts the access of high molecular weight inhibitors to the opening (Brohawn *et al.*, 2012; Miller and Long, 2012).

We previously demonstrated that low micromolar concentrations of ruthenium red ($[(NH_3)_5Ru\text{-}O\text{-}Ru(NH_3)_4\text{-}O\text{-}Ru(NH_3)_5]Cl_6$) inhibit TASK-3 background K^+ channel, whereas TASK-1 is not affected by the polycationic dye (Czirják and Enyedi, 2003). This observation proved to be useful because of the remarkably selective action of ruthenium red (RR) distinguishing between the two closely related TASK channels, and despite of the limited overall specificity of the compound. RR is known to inhibit a multitude of target proteins, most of them related to the transport or binding of Ca^{2+} (e.g. calcium channels and pumps, as detailed in the Discussion section of ref. (Czirják and Enyedi, 2003)). A negatively charged amino acid, glutamate 70 (E70) was established as the major determinant of TASK-3 inhibition by RR

(Czirják and Enyedi, 2003; Musset *et al.*, 2006; Gonzalez *et al.*, 2013). TASK-1 contains a positive lysine in the corresponding position, and the channel was rendered RR-sensitive by the K70E mutation, indicating that the high charge density ruthenium compound differentiated between the channels by electrostatic interaction on the basis of a single distinct amino acid residue.

Differential sensitivity of TASK-1 and TASK-3 to RR has been extensively used to investigate TASK currents in adrenal glomerulosa cells (Czirják and Enyedi, 2002b), carotid body glomus cells (Kim *et al.*, 2009), cardiomyocytes (Putzke *et al.*, 2007), pulmonary artery smooth muscle cells (Olschewski *et al.*, 2006), motoneurons (Berg *et al.*, 2004; Larkman and Perkins, 2005), cerebellar granule neurons (Lauritzen *et al.*, 2003; Kang *et al.*, 2004; Aller *et al.*, 2005), thalamocortical relay neurons (Musset *et al.*, 2006), and several other cell types (Berg and Bayliss, 2007; Deng and Lei, 2008; Weber *et al.*, 2008; Ernest *et al.*, 2010). We reported previously that in addition to TASK-3, another K2P channel, TRAAK, a member of the TREK subfamily, is also sensitive to RR. Whereas in the case of TASK-3 the Hill coefficient of about 1 was in good accordance with the binding of one RR molecule simultaneously to both E70 residues in the dimer of the subunits, the inhibition of TRAAK by RR was characterized by a Hill coefficient of 2, suggesting that RR inhibits TRAAK and TASK-3 by different mechanisms (Czirják and Enyedi, 2002a).

In the present study we investigated a more comprehensive set of K2P channels in order to categorize them into RR-sensitive and RR-resistant groups, and also examined the mechanism of action of the inhibitor.

METHODS

Plasmids and reagents

The cloning of mouse TASK-1/2/3 (K2P3.1/K2P5.1/K2P9.1), TREK-2 (K2P10.1), TALK-1 (K2P16.1), THIK-1 (K2P13.1) and human and mouse TRESK (K2P18.1) has been described previously (Czirják and Enyedi, 2006; Czirják *et al.*, 2004). Human and mouse TRAAK (K2P4.1) and TREK-1 (K2P2.1), and human TREK-2 channel plasmids were kindly provided by Professor M. Lazdunski and Dr. F. Lesage. Drug target nomenclature conforms with British Journal of Pharmacology's Guide to Receptors and Channels (Alexander *et al.*, 2013). Different mutant versions of these channels were produced with QuikChange site-directed mutagenesis kit (Stratagene, La Jolla, CA) according to the manufacturer's instructions. For the construction of tandem wt/wt, wt/mutant and mutant/wt mTREK-2 channels, the TAA stop codon of the upstream subunit and the ATG start codon of the downstream subunit were replaced with a unique MunI restriction enzyme site. This introduced a two amino acid linker (glutamine and leucine) between the coding sequences of the concatenated subunits.

Chemicals of analytical grade were purchased from Sigma (St. Louis, MO), Fluka (Milwaukee, WI) or Merck (Whitehouse Station, NJ). Enzymes and kits for molecular biology applications were purchased from Ambion (Austin, TX), Thermo Scientific (Waltham, MA), New England Biolabs (Beverly, MA) and Stratagene.

Purification of ruthenium violet

Ruthenium red (RR) and ruthenium violet (RV) were dissolved in 0.1 M ammonium acetate

as 10 mM stock solutions, and diluted further in high [K^+] solution before the measurement. In order to purify RV, we applied cation exchange chromatography using carboxy-methyl (CM) cellulose resin (Whatman CM52). Crude RR preparation (70 mg) was dissolved in ammonium acetate (AA, 10 mM, 30 ml). The solution was applied to a 1 ml CM cellulose column at a flow rate of 0.4 ml/min. The flowthrough was colorless, whereas the column became dark with the adsorbed dyes. Bulk RR was eluted by two rounds of isocratic elution (750 mM AA, 10 ml), followed by washing steps (50 mM AA, 20 ml). Subsequently, RV was eluted with a linear gradient of AA (from 50 mM to 1.5 M, in 20 ml); the major RV peak appeared between 1.2-1.4 M. Fractions containing RV were lyophilized, immediately dissolved in 10 mM AA, and stored at -20 °C. The calculated molar ratio of RV/RR was increased from 0.1 to 9.5 by the purification. (RV concentration was calculated using the extinction coefficient $\varepsilon = 311$ $(g/100\ ml)^{-1}cm^{-1}$ at 734 nm (Luft, 1971), and molecular weight 751.43 g/mol (Hall and Griffith, 1980)).

Animals, Xenopus oocyte microinjection, isolation of DRG neurons

DRG neurons derived from six NMRI mice, purchased from Toxicoop, Budapest, Hungary. Mice were maintained on a 12 h light/dark cycle with free access to food and water. Animals were sacrificed by CO_2 exposure. *Xenopus* oocytes were prepared, the cRNA was synthesized and microinjected as previously described (Czirják *et al.*, 2004). (For the expression of the different channel types, 57 pg - 2.3 ng/oocyte cRNA was injected.) Fifteen frogs were used for the experiments. The animals were maintained in two 50 L tanks, with continuous filtering and water circulation through aquarium pumps at 19 °C in an air conditioned room. The frogs were anaesthetized with 0.1% tricaine solution and sacrificed by decerebration and pithing. All

treatments of the animals were conducted in accordance with state laws and institutional regulations. The experiments were approved by the Animal Care and Ethics Committee of Semmelweis University (approval ID: XIV-I-001/2154-4/2012). The results of all studies involving animals are reported in accordance with the ARRIVE guidelines (McGrath *et al.*, 2010).

Dorsal root ganglia (DRGs) were dissected from thoracic and lumbar levels of the spinal cord of 40-70 day old mice. DRGs were collected in sterile PBS (137 mM NaCl, 2.7 mM KCl, 10 mM NaH_2PO_4, pH 7.4 with NaOH) at 4°C. Ganglia were incubated with gentle shaking for 30 min at 37 °C in PBS containing 2 mg/ml collagenase (type I; Worthington, Lakewood, NJ). Then DMEM-F-12 containing 10 % fetal bovine serum (Lonza, Basel, Switzerland) and 100 U/ml penicillin-streptomycin (Sigma) was added, and gentle trituration was performed with a cut 1 ml plastic pipette tip for 10-15 times. Cells were centrifuged at 200 g for 5 minutes, washed three times with culture medium, and plated on plastic culture dishes treated with poly-L-lysine. They were incubated in 95% air - 5% CO_2 mixture at 37 °C, and measured after 1-3 days.

Two-electrode voltage clamp and patch clamp measurements

Two-electrode voltage clamp experiments were performed three or four days after the microinjection of cRNA, as previously described (Czirják *et al.*, 2004). Low [K^+] solution contained (in mM): NaCl 95.4, KCl 2, $CaCl_2$ 1.8, HEPES 5 (pH 7.5 adjusted with NaOH). High [K^+] solution contained 80 mM K^+ (78 mM Na^+ of the low [K^+] solution was replaced with K^+). Background K^+ currents were measured at the end of 300 ms long voltage steps to -100 mV applied in every 4 s.

DRG neurons were measured by whole-cell patch clamp at 37 °C. The low [K^+] extracellular

solution contained (in mM): NaCl 140, KCl 2, $MgCl_2$ 0.5, $CaCl_2$ 2, glucose 11, HEPES 10, pH 7.4 (adjusted with NaOH). High [K^+] extracellular solution contained 30 mM K^+ (28 mM Na^+ of the low [K^+] solution was replaced with K^+). Pipettes were pulled from borosilicate glass by a P-87 puller (Sutter Instrument Co., Novato, CA) and fire polished. Pipette resistance ranged between 3 and 9 MΩ when filled with the intracellular solution containing (in mM): KCl 135, $MgCl_2$ 2, EGTA 1, Na_2ATP 2, HEPES 10, pH 7.3 (adjusted with NaOH). The pipette was connected to the headstage of a patch clamp amplifier Axopatch-1D (Axon Instruments, Inc., Foster City, CA), data were digitally sampled by Digidata 1200 (Axon Instruments), and analyzed by pCLAMP 10 software (Molecular Devices, Sunnyvale, CA).

Statistics and calculations

Data are expressed as means±S.E. Normalized dose-response curves were fitted by a modified Hill equation of the form $y = \alpha / (1 + (c/K_{1/2})^n) + (1 - \alpha)$, where c is the concentration, $K_{1/2}$ is the concentration at which half-maximal inhibition occurs, n is the Hill coefficient, and α is the fraction inhibited by the treatment. Statistical significance was estimated by Student's t test for independent samples, one-way ANOVA followed by Scheffe's post hoc test or Pearson's product-moment correlation analysis (as indicated in the figure legends). The difference was considered to be significant at $p<0.05$.

RESULTS

Characterization of the ruthenium red sensitivity of K_{2P} channels: TREK-2 is potently inhibited by the polycationic compound

Different K2P channel types were expressed in *Xenopus laevis* oocytes, and their sensitivity to the polycationic dye ruthenium red (RR, Fig. 1. A) was measured at -100 mV in 80 mM [K^+] by two-electrode voltage clamp. In accordance with our previous results (Czirják and Enyedi, 2002a), human and mouse TREK-1 (K2P2) currents were negligibly affected by the application of 10 μM RR (for representative recording see Fig. 1. B). Neither of our RR preparations, purchased from Sigma in 1996 and 2013, respectively, were effective inhibitors of TREK-1. RR_{2013} reduced human TREK-1 current only by 5.0 ± 1.9 % (n = 5), and the mouse channel current by 7.1 ± 2.4 % (n = 6; see *hTREK-1* and *mTREK-1* in Fig. 1. E). Unexpectedly, human and mouse TREK-2 (K2P10) currents were substantially blocked by RR, despite of the high amino acid sequence similarity of TREK-1 and TREK-2 channels (for representative recording see Fig. 1. C). Human TREK-2 was inhibited by 75.1 ± 4.2 % (n = 4), whereas its mouse counterpart by 90.7 ± 1.6 % (n = 6; see *hTREK-2* and *mTREK-2* in Fig. 1. E). RR_{1996} similarly inhibited TREK-2 as RR_{2013} (*not shown*). These data indicate that in addition to its discriminating effect on TASK channels, ruthenium red also distinguishes between the closely related TREK-1 and TREK-2 members of the K2P family.

The third member of the TREK subfamily, TRAAK (K2P4), was less inhibited by 10 μM RR_{2013} than TREK-2 (for representative recording see Fig. 1. D; 32.3 ± 2.7 % (n = 5) and 56.0 ± 0.7 % (n = 8) inhibition for human and mouse TRAAK, respectively, Fig. 1. E). This relatively weak inhibition of TRAAK by RR was not anticipated, because of our own previously reported

data about the high sensitivity of the channel to RR (Czirják and Enyedi, 2002a), and urged us to investigate the reason for the apparent discrepancy between the present and previous data (*see below*). Among the other tested K2P channels, mouse TASK-3 was inhibited (Fig. 1. E) as reported previously (Czirják and Enyedi, 2003), whereas mTALK-1, mTASK-1, mTASK-2, mTHIK-1 and mTRESK (and hTRESK) were not sensitive to the polycation (less than 10 % inhibition, Fig. 1. E).

Aspartate 135 (D135) in the extracellular ion pathway (EIP) of TREK-2 is responsible for the inhibition by ruthenium red

Since the RR-sensitivity of TREK-2 is reported for the first time, we analyzed this inhibitory effect in more detail. RR inhibited TREK-2 with a half-maximal inhibitory concentration of 0.23 ± 0.06 μM (Fig. 2). Hill coefficient was 1.2 ± 0.3, suggesting that a single RR molecule interacted with the functional dimer. The rapid onset of the inhibition (Fig. 1. C) suggested that the RR-binding site of TREK-2 is extracellular, in good accordance with the limited permeation of the polycationic compound through the plasma membrane.

In order to identify the amino acids interacting with the RR molecule, we mutated negatively charged and histidine residues of TREK-2 in the first extracellular loop, where the sequence of TREK-2 differed from the RR-resistant TREK-1 (Fig. 3. A). We changed these amino acids in combinations or one-by-one to the corresponding residues of TREK-1, and tested the sensitivity of the constructs to 10 μM RR (Fig. 3. B and C). D115Q, H130Q and E108Q-E111T double mutants were inhibited by RR, similarly to the wild type channel. In sharp contrast, the D133A-D135I double mutant was resistant to the inhibitor. (Mouse TREK-2c was used (Mirkovic and

Wickman, 2011); the ALDADNA sequence is also conserved in other splice variants.) Next, we examined the individual contribution of D133 and D135 to the inhibitory effect. The D133A construct was similarly sensitive to RR as the wild type channel, but RR did not inhibit the D135I mutant (Fig. 3. B and C). Thus D135 is the major determinant of the inhibition of TREK-2 by RR.

Since K2P channels function as dimers, we examined whether D135 of both subunits were necessary for the inhibition. We designed a tandem (concatenated) construct and expressed the two TREK-2 subunits as a continuous polypeptide (Fig. 3. D). Tandem TREK-2 was similarly sensitive to RR as the wild type channel (81.8 ± 3.1 % inhibition, n = 6, Fig. 3. D). Mutation of D135 in the N- or C-terminal half of the tandem construct reduced the sensitivity to RR (34.7 ± 3.1 % (n = 6) and 48.2 ± 5.9 % (n = 6) inhibition for *wt/D135I* and *D135I/wt* channels by 10 μM RR, respectively, Fig. 3. D). Thus the D135 residues of both subunits contribute to the effect, although one intact D135 still allowed the inhibition by RR to some extent.

As discussed above, TREK-1 is resistant to RR (Fig. 1. B and E). Because TREK-1 has isoleucine (I110) in the position corresponding to D135 of TREK-2, we replaced this hydrophobic residue with the acidic aspartate. As opposed to the wild-type channel, the I110D point mutant of TREK-1 was substantially inhibited by 10 μM RR (79.5 ± 1.7 % inhibition (n = 6); Fig. 3. E). The introduction of the aspartate to the appropriate position was sufficient to create a RR binding site even in the molecular context of TREK-1.

Ruthenium violet inhibits TRAAK more potently than RR

Mouse TRAAK appeared to be less inhibited by RR in this study than we previously reported

(Czirják and Enyedi, 2002a). An old commercial preparation of RR (Sigma 1996) evoked qualitatively different effect on TRAAK from that of our present RR batch (Sigma 2013, Fig. 4). In addition to the higher efficacy of RR_{1996}, the old product also inhibited TRAAK with slower kinetics than the new one. Mouse TRAAK was more efficiently inhibited by both RR preparations than the human ortholog, however, the slow kinetics of inhibition by RR_{1996} was apparent irrespective of the species (Fig. 4).

It is known that commercial preparations of RR may contain contaminants, e.g. ruthenium ammine compounds (with absorption maxima between 200 and 400 nm), and ruthenium violet (RV, absorption peaks at 734 and 900 nm, see ref. (Luft, 1971)). In the absorption spectra of equal mass concentration of RR_{1996} and RR_{2013}, the peak amplitudes at 533 nm, characteristic for RR, were different (Fig. 5. A). RR_{1996} preparation contained less ruthenium red than RR_{2013}, despite of the more pronounced inhibition of TRAAK by the older preparation. Therefore we concluded that contaminants in the RR_{1996} sample also inhibit TRAAK in addition to RR. (Where not specified otherwise, RR_{2013} of high purity was used throughout this study.)

Since a small absorption peak at 734 nm was present in RR_{1996} but not in RR_{2013} (Fig. 5. A), we examined whether ruthenium violet (RV, $[Ru_3N_2(NH_3)_8(OH)(OH_2)_5]Cl_5$) inhibits TRAAK (Hall and Griffith, 1980). To this end, we purified RV by ion exchange chromatography using a low charge density CM-cellulose column (see *Methods*, and Fig. 5.A for the spectrum of purified RV). Ruthenium violet inhibited TRAAK with higher potency than ruthenium red (IC_{50} value of 0.11 ± 0.01 and 1.7 ± 0.1 μM for RV and $RR_{(2013)}$, respectively, Fig. 5. B). Hill coefficients for RR and RV were 1.1 ± 0.1 and 2.0 ± 0.3, respectively, suggesting that the mechanisms of action of the two ruthenium compounds on TRAAK are different. TRAAK dimer may contain two binding sites for RV, but only one for RR. Reconstitution of the absorption maxima of RR_{1996} at 533 and 734 nm by mixing RR_{2013} with purified RV indicated that RV was partly responsible for

the difference of inhibition of mTRAAK by the two RR preparations (see *supplementary material*). Our results suggest that RV is a more potent inhibitor of TRAAK than RR, and the effect of some commercial preparations of RR may also depend on their RV contamination in addition to their RR content.

The effect of RV was also tested on a more extensive set of K2P channels (Fig. 5. C). The inhibitory profiles of RR (Fig. 1. E) and RV (Fig. 5. C) turned out to be similar. The D135I mutation also prevented the inhibitory effect of RV (Fig. 5. C), suggesting a common site of action of RR and RV in the case of TREK-2 channel.

RR-sensitive background potassium current in DRG neurons

Dorsal root ganglion (DRG) neurons have been reported to express predominantly TREK-2 and the RR-insensitive TREK-1 and TRESK background K^+ channels in rodents (Talley *et al.*, 2001; Kang and Kim, 2006; Dobler *et al.*, 2007). We performed whole cell patch clamp recordings on mouse DRG neurons at 37 °C to investigate the RR-sensitive and temperature-dependent TREK-2 current (Kang *et al.*, 2005; Pereira *et al.*, 2014). In a representative neuron, RR (10 μM) inhibited the K^+ current by 71 % at -100 mV in 30 mM extracellular [K^+], and the outward current was also reduced at positive potentials in accordance with the leak characteristics of the blocked current component (Fig. 6. A-C; voltage-gated K^+ channels dominated the outward current). High sensitivity to RR is compatible with the predominant contribution of TREK-2 to the background potassium current in this neuron. (The reversal potential of the difference current (Fig. 6. B) closely approximates the calculated equlibrium potential of K^+ (-40 mV in 30 mM

[K^+] at 37 °C). RR also inhibited a small voltage-dependent component (between -60 and -40 mV), the ion selectivity of which has not been further examined. The saturation effect of the difference current above +20 mV may be related to the voltage-dependent nature of the inhibition by the cationic dye.)

We examined RR-sensitivity of the K^+ currents of 20 DRG neurons with diameters in the range of 16-45 µm. The amplitudes of the K^+ currents (the differences of inward currents in 2 and 30 mM extracellular [K^+] at -100 mV) were between 120 and 2540 pA. The effect of RR varied considerably in this cell population, from complete insensitivity to about 75 % inhibition (Fig. 6. D). We found weak negative correlation between the K^+ current amplitude and the RR-sensitivity ($r = -0.6$, $p < 0.005$), suggesting that neurons with large K^+ current at -100 mV expressed relatively less TREK-2.

DISCUSSION

K2P background K^+ channels are the major determinants and regulators of the resting membrane potential in several cell types (Enyedi and Czirják, 2010). However, the pharmacological separation of their almost identical macroscopic currents have not yet been adequately resolved. In the absence of specific inhibitors, the pharmacological tools aiding the discrimination of the currents of different K2P channels are appreciated. This explains that the otherwise relatively non-specific ruthenium red (RR) has been extensively used to distinguish between TASK-1 and TASK-3 currents.

In the present study we demonstrate that RR also discriminates between TREK-1 and TREK-2 channels. In fact, this finding is so counter-intuitive that in a recent report, the RR-insensitivity of TREK-2 has been anticipated because TREK-1 is not affected by the compound (Cadaveira-Mosquera *et al.*, 2011). However, RR can distinguish between target proteins depending on a single amino acid difference (per subunit), and such a decisive variation of sequence is present not only in the TASK channels but also in the two closely related members of the TREK subfamily. The negatively charged aspartate 135 mediates the inhibition of TREK-2 by RR, in sharp contrast to the RR-resistant TREK-1 containing the hydrophobic isoleucine 110 in the corresponding position.

The outer entrance of the ion conducting pore of K2P channels is covered by an extracellular cap domain, as recently revealed by the crystal structures of TWIK-1 (PDB ID: 3UKM; (Miller and Long, 2012)), TRAAK (PDB ID: 3UM7 and 4I9W; (Brohawn *et al.*, 2012; Brohawn *et al.*, 2013)), and TREK-2 (PDB ID: 4BW5). A short tunnel piercing through the extracellular cap, roughly parallel to the plane of the plasma membrane, the so-called extracellular ion pathway (EIP) connects the extracellular space to the pore entrance. (The EIP and the pore together form a

T shape, where the horizontal line of the "T" is the EIP, whereas the vertical line corresponds to the pore through the plasma membrane.) D135 residues are located in the middle of the EIP, on the ceiling of the tunnel, just above the selectivity filter, in symmetrical arrangement (Fig. 7). We propose that this junction region between the EIP and the pore entrance is the binding site of RR, where the inhibitor can electrostatically and/or sterically hinder the movement of the charge carrier. D135 residue, identified in the present study, is located at a position of the EIP that is similar, or maybe even, identical to E70 of TASK-3 (Czirják and Enyedi, 2003; Gonzalez *et al.*, 2013). The exact position of D135 of TREK-2 and E70 of TASK-3 relative to the EIP appears to be slightly different (compare Fig. 7 to Fig. 1 in the Gonzalez *et al.*, 2013 reference), however, it remains a question how faithfully the static structure distorted into a protein crystal represents the fine details of side chain arrangements in the functional channels. The conditions of crystallization may have drastic effects on the conformation of K2P channels as exemplified by the different reported structures of TRAAK (Brohawn *et al.*, 2012; Brohawn *et al.*, 2013).

TREK channels are regulated in a highly complex manner, and most of the regulatory properties are shared by TREK-1 and TREK-2. Both channels are mechanosensitive, temperature-dependent, activated by intracellular acidification, volatile anesthetics and polyunsaturated fatty acids, and inhibited by protein kinase A, C and AMP-activated protein kinase (Enyedi and Czirják, 2010). Although most properties of TREK-1 and TREK-2 are identical, some differences between them have also been reported. Extracellular acidification inhibits TREK-1, but activates TREK-2, depending on the protonation of a conserved histidine residue in the first extracellular loop of the channels (Sandoz *et al.*, 2009; Bagriantsev *et al.*, 2011). The two TREK channels can also be distinguished on the basis of their different single-channel conductance, however, this approach is complicated by the multiple conductance levels arising from alternative translation initiation variants (Thomas *et al.*, 2008; Simkin *et al.*, 2008).

TREK-1 and TREK-2 are differentially expressed in the central nervous system and also at the periphery, suggesting that the two apparently similar channel types may have different functions (for review, see (Noel *et al.*, 2011)). Ruthenium red distinguishes between the macroscopic currents of TREK-1 and TREK-2, and may complement the presently available methodological repertoire for the discrimination of the two channel types.

Ruthenium red also inhibits the third member of the TREK subfamily, TRAAK, although less efficiently than we originally reported (Czirják and Enyedi, 2002a). Despite of its lower pure RR content, RR_{1996} preparation was a more effective inhibitor of TRAAK than RR_{2013}. Ruthenium violet (RV) also contributed to the inhibition of TRAAK by the old preparation. The different Hill coefficients for RR and RV suggest that not only their affinities to TRAAK but also the mechanisms of action of the two ruthenium compounds are different. It is probable that RR and RV also inhibit TRAAK by binding to negatively charged extracellular regions of the channel, however, the identification of these binding sites is not straightforward. Mouse TRAAK subunit contains 14 negatively charged (Asp and Glu) and 5 histidine (His) residues in its extracellular loops. The sequence alignments of TRAAK with the TREK channels and the crystal structures are not particularly helpful for the prediction of the regions responsible for the interaction. Therefore a comprehensive mutational screening approach will be required in the future to determine which amino acids constitute the RR and RV binding sites of TRAAK.

Dorsal root ganglion (DRG) neurons express several K2P channel types, as detected by in situ hybridization (Talley *et al.*, 2001). The contribution of different channels to the ensemble background K^+ current was estimated by single channel analysis (Kang and Kim, 2006). TREK-2 was suggested to contribute 69 % to the background K^+ current at 37 °C, followed by TRESK (16 %), TREK-1 (12 %), and TRAAK (3 %). In a recent report, TREK-2 was immunodetected in a high number of DRG neurons, and small DRG neurons were found to contain higher TREK-2

immunoreactivity than the large cells (Acosta *et al.*, 2014).

We were curious whether we can detect the ruthenium red sensitive TREK-2 current component by whole-cell patch clamp measurements in isolated DRG neurons. In several cells, characterized by relatively small (< 0.5 nA) K^+ current amplitudes at -100 mV in high (30 mM) [K^+], RR inhibited the current by 60-70 %. This strong inhibition by RR is consistent with high TREK-2 expression, and is in good accordance with the previous immunocytochemistry data that small cells express TREK-2 most abundantly (Acosta *et al.*, 2014). Evidently, TRAAK and TASK-3 may have also contributed to the current inhibited by RR, although previous reports suggest that TREK-2 is predominant. On the other hand, in some neurons, characterized by relatively large (> 0.5 nA) K^+ current amplitudes, the background potassium current was weakly (< 20 %) inhibited by RR, indicating that in these cells TREK-2 (as well as TRAAK and TASK-3) were minor components. In summary, we provided the first data about the contribution of TREK-2 to the whole-cell background potassium current of individual DRG neurons, and our results suggest that ruthenium red can also be applied for the verification of TREK-2 current in other native cell types.

ACKNOWLEDGMENTS

This work was supported by the Hungarian National Research Fund (OTKA K108496). The skillful technical assistance of Alice Dobolyi and Irén Veres is acknowledged.

AUTHOR CONTRIBUTIONS

Conceived and designed the experiments: GB ML PE GC.

Performed the experiments: GB ML PE GC.

Analyzed the data: GB ML PE GC.

Wrote the paper: GB ML PE GC.

CONFLICT OF INTEREST

None.

REFERENCES

Acosta C, Djouhri L, Watkins R, Berry C, Bromage K, Lawson SN (2014). TREK2 expressed selectively in IB4-binding C-fiber nociceptors hyperpolarizes their membrane potentials and limits spontaneous pain. *J Neurosci* **34**: 1494-1509.

Alexander SP, Benson HE, Faccenda E, Pawson AJ, Sharman JL, McGrath JC *et al.* (2013). The Concise Guide to PHARMACOLOGY 2013/14: overview. *Br J Pharmacol* **170**: 1449-1458.

Aller MI, Veale EL, Linden AM, Sandu C, Schwaninger M, Evans LJ *et al.* (2005). Modifying the subunit composition of TASK channels alters the modulation of a leak conductance in cerebellar granule neurons. *J Neurosci* **25**: 11455-11467.

Bagriantsev SN, Peyronnet R, Clark KA, Honore E, Minor DL, Jr. (2011). Multiple modalities converge on a common gate to control K2P channel function. *EMBO J* **30**: 3594-3606.

Berg AP, Bayliss DA (2007). Striatal cholinergic interneurons express a receptor-insensitive homomeric TASK-3-like background K^+ current. *J Neurophysiol* **97**: 1546-1552.

Berg AP, Talley EM, Manger JP, Bayliss DA (2004). Motoneurons express heteromeric TWIK-related acid-sensitive K^+ (TASK) channels containing TASK-1 (KCNK3) and TASK-3 (KCNK9) subunits. *J Neurosci* **24**: 6693-6702.

Bittner S, Budde T, Wiendl H, Meuth SG (2010). From the background to the spotlight: TASK channels in pathological conditions. *Brain Pathol* **20**: 999-1009.

Brohawn SG, Campbell EB, MacKinnon R (2013). Domain-swapped chain connectivity and gated membrane access in a Fab-mediated crystal of the human TRAAK K^+ channel. *Proc Natl Acad Sci U S A* **110**: 2129-2134.

Brohawn SG, del Marmol J, MacKinnon R (2012). Crystal structure of the human K2P TRAAK, a lipid- and mechano-sensitive K^+ ion channel. *Science* **335**: 436-441.

Cadaveira-Mosquera A, Ribeiro SJ, Reboreda A, Perez M, Lamas JA (2011). Activation of TREK currents by the neuroprotective agent riluzole in mouse sympathetic neurons. *J Neurosci* **31**: 1375-1385.

Czirják G, Enyedi P (2002a). Formation of functional heterodimers between the TASK-1 and TASK-3 two-pore domain potassium channel subunits. *J Biol Chem* **277**: 5426-5432.

Czirják G, Enyedi P (2002b). TASK-3 dominates the background potassium conductance in rat adrenal glomerulosa cells. *Mol Endocrinol* **16**: 621-629.

Czirják G, Enyedi P (2003). Ruthenium red inhibits TASK-3 potassium channel by interconnecting glutamate 70 of the two subunits. *Mol Pharmacol* **63**: 646-652.

Czirják G, Enyedi P (2006). Zinc and mercuric ions distinguish TRESK from the other two-pore-

domain K^+ channels. *Mol Pharmacol* **69**: 1024-1032.

Czirják G, Tóth ZE, Enyedi P (2004). The two-pore domain K^+ channel, TRESK, is activated by the cytoplasmic calcium signal through calcineurin. *J Biol Chem* **279**: 18550-18558.

Deng PY, Lei S (2008). Serotonin increases GABA release in rat entorhinal cortex by inhibiting interneuron TASK-3 K^+ channels. *Mol Cell Neurosci* **39**: 273-284.

Dobler T, Springauf A, Tovornik S, Weber M, Schmitt A, Sedlmeier R *et al.* (2007). TRESK two-pore-domain K^+ channels constitute a significant component of background potassium currents in murine dorsal root ganglion neurones. *J Physiol* **585**: 867-879.

Enyedi P, Czirják G (2010). Molecular background of leak K^+ currents: two-pore domain potassium channels. *Physiol Rev* **90**: 559-605.

Ernest NJ, Logsdon NJ, McFerrin MB, Sontheimer H, Spiller SE (2010). Biophysical properties of human medulloblastoma cells. *J Membr Biol* **237**: 59-69.

Gonzalez W, Zuniga L, Cid LP, Arevalo B, Niemeyer MI, Sepulveda FV (2013). An extracellular ion pathway plays a central role in the cooperative gating of a K(2P) K^+ channel by extracellular pH. *J Biol Chem* **288**: 5984-5991.

Hall JP, Griffith WP (1980). Studies on transition-metal nitrido- and oxo-complexes. Part 6. Nitrido-bridged complexes of osmium and ruthenium . *J Chem Soc , Dalton Trans*: 2410-2414.

Humphrey W, Dalke A, Schulten K (1996). VMD: visual molecular dynamics. *J Mol Graph* **14**: 33-38.

Kang D, Choe C, Kim D (2005). Thermosensitivity of the two-pore domain K^+ channels TREK-2 and TRAAK. *J Physiol* **564**: 103-116.

Kang D, Han J, Talley EM, Bayliss DA, Kim D (2004). Functional expression of TASK-1/TASK-3 heteromers in cerebellar granule cells. *J Physiol* **554**: 64-77.

Kang D, Kim D (2006). TREK-2 (K2P10.1) and TRESK (K2P18.1) are major background K^+ channels in dorsal root ganglion neurons. *Am J Physiol Cell Physiol* **291**: C138-C146.

Kim D, Cavanaugh EJ, Kim I, Carroll JL (2009). Heteromeric TASK-1/TASK-3 is the major oxygen-sensitive background K^+ channel in rat carotid body glomus cells. *J Physiol* **587**: 2963-2975.

Larkman PM, Perkins EM (2005). A TASK-like pH- and amine-sensitive 'leak' K^+ conductance regulates neonatal rat facial motoneuron excitability in vitro. *Eur J Neurosci* **21**: 679-691.

Lauritzen I, Zanzouri M, Honore E, Duprat F, Ehrengruber MU, Lazdunski M *et al.* (2003). K^+-dependent cerebellar granule neuron apoptosis. Role of task leak K^+ channels. *J Biol Chem* **278**: 32068-32076.

Lotshaw DP (2007). Biophysical, pharmacological, and functional characteristics of cloned and

native mammalian two-pore domain K^+ channels. *Cell Biochem Biophys* **47**: 209-256.

Luft JH (1971). Ruthenium red and violet. I. Chemistry, purification, methods of use for electron microscopy and mechanism of action. *Anat Rec* **171**: 347-368.

Mathie A, Veale EL (2007). Therapeutic potential of neuronal two-pore domain potassium-channel modulators. *Curr Opin Investig Drugs* **8**: 555-562.

McGrath JC, Drummond GB, McLachlan EM, Kilkenny C, Wainwright CL (2010). Guidelines for reporting experiments involving animals: the ARRIVE guidelines. *Br J Pharmacol* **160**: 1573-1576.

Miller AN, Long SB (2012). Crystal structure of the human two-pore domain potassium channel K2P1. *Science* **335**: 432-436.

Mirkovic K, Wickman K (2011). Identification and characterization of alternative splice variants of the mouse Trek2/Kcnk10 gene. *Neuroscience* **194**: 11-18.

Musset B, Meuth SG, Liu GX, Derst C, Wegner S, Pape HC *et al.* (2006). Effects of divalent cations and spermine on the K^+ channel TASK-3 and on the outward current in thalamic neurons. *J Physiol* **572**: 639-657.

Noel J, Sandoz G, Lesage F (2011). Molecular regulations governing TREK and TRAAK channel functions. *Channels (Austin)* **5**: 402-409.

Olschewski A, Li Y, Tang B, Hanze J, Eul B, Bohle RM *et al.* (2006). Impact of TASK-1 in human pulmonary artery smooth muscle cells. *Circ Res* **98**: 1072-1080.

Pereira V, Busserolles J, Christin M, Devilliers M, Poupon L, Legha W *et al.* (2014). Role of the TREK2 potassium channel in cold and warm thermosensation and in pain perception. *Pain*., *in press*

Putzke C, Wemhoner K, Sachse FB, Rinne S, Schlichthorl G, Li XT *et al.* (2007). The acid-sensitive potassium channel TASK-1 in rat cardiac muscle. *Cardiovasc Res* **75**: 59-68.

Sandoz G, Douguet D, Chatelain F, Lazdunski M, Lesage F (2009). Extracellular acidification exerts opposite actions on TREK1 and TREK2 potassium channels via a single conserved histidine residue. *Proc Natl Acad Sci U S A* **106**: 14628-14633.

Simkin D, Cavanaugh EJ, Kim D (2008). Control of the single channel conductance of K2P10.1 (TREK-2) by the amino-terminus: role of alternative translation initiation. *J Physiol* **586**: 5651-5663.

Talley EM, Solorzano G, Lei Q, Kim D, Bayliss DA (2001). Cns distribution of members of the two-pore-domain (KCNK) potassium channel family. *J Neurosci* **21**: 7491-7505.

Thomas D, Plant LD, Wilkens CM, McCrossan ZA, Goldstein SA (2008). Alternative translation initiation in rat brain yields K2P2.1 potassium channels permeable to sodium. *Neuron* **58**: 859-

870.

Weber M, Schmitt A, Wischmeyer E, Doring F (2008). Excitability of pontine startle processing neurones is regulated by the two-pore-domain K^+ channel TASK-3 coupled to 5-HT2C receptors. *Eur J Neurosci* **28**: 931-940.

Yaffe E, Fishelovitch D, Wolfson HJ, Halperin D, Nussinov R (2008). MolAxis: a server for identification of channels in macromolecules. *Nucleic Acids Res* **36**: W210-W215.

LEGEND TO FIGURES

Fig. 1. TREK-2, TRAAK and TASK-3 are blocked by ruthenium red.

A. Chemical structure and molecular formula of ruthenium red (RR). **B.** Representative two-electrode voltage clamp recording from a *Xenopus* oocyte expressing mouse TREK-1. After the rundown of TREK-1 current at the beginning of the measurement, two ruthenium red preparations were administered (RR_{2013} and RR_{1996} from Sigma, as indicated by the *colored horizontal bars*). TREK-1 has not been affected by ruthenium red (10 μM). The current was measured at -100 mV and the extracellular [K^+] was changed from 2 to 80 mM and back as shown *above* the recording. **C.** The sensitivity of mouse TREK-2 channel to ruthenium red (RR_{2013}) was tested as in panel A. Ruthenium red (10 μM) strongly inhibited TREK-2 current. **D.** Representative recording of mouse TRAAK current inhibition by RR_{2013} (10 μM). The inhibition of TRAAK was intermediate between TREK-1 and TREK-2. **E.** Ruthenium red sensitivity of K2P channels (as indicated *below* the *column graph*) is illustrated. In addition to the positive control mouse TASK-3 (mTASK-3), human and mouse TREK-2 (hTREK-2 and mTREK-2) currents were also diminished by RR, whereas human and mouse TRAAK currents were less inhibited. TREK-1, TALK-1, TASK-1, TASK-2, THIK-1 and TRESK were not affected by RR. (Where not specified otherwise, RR_{2013} of high purity was used in the experiments. All oocyte measurements were performed at room temperature (21 °C).)

Fig. 2. Dose-response relationship of TREK-2 current and ruthenium red concentration.

Mouse TREK-2 currents were measured in high (80 mM) [K^+] at -100 mV in the presence of different (0.03, 0.1, 0.3, 1, 3 and 10 μM) concentrations of ruthenium red. The currents were

corrected for the small nonspecific leak in 2 mM extracellular [K^+] and normalized to the value without the inhibitor. Each data point represents the average of normalized currents of six to nine oocytes. The data points were fitted by a modified Hill equation (see *Methods*).

Fig. 3. Mutation of aspartate 135 (D135) to isoleucine eliminates RR-sensitivity of TREK-2, whereas the substitution of isoleucin 110 (I110) in TREK-1 with aspartate confers RR-sensitivity to the channel.

A. Sequence alignment of a region of different K2P channels (as indicated on the *left*) between the first transmembrane segment and the first pore domain. In this region, TREK-2 contains additional negatively charged or histidine residues, compared to TREK-1 (as indicated with *yellow* and *green*). D135 residue of TREK-2, corresponding to the RR-binding E70 amino acid of TASK-3, is indicated with *red* and *cyan*. **B.** Represenative recordings of mouse wild type (*wt*), D135I and D133A mutant TREK-2 currents and their sensitivity to RR were measured similarly as in panel C of Fig. 1. **C.** Sensitivity of wild type (*wt*) and different mutant versions of mouse TREK-2 (as indicated *below* the column diagram) to ruthenium red (10 μM). Negatively charged and histidine amino acids of TREK-2 were replaced by the corresponding (non-conserved) residues of the RR-resistant TREK-1. The current in the presence of RR was normalized to the initial value without the inhibitor. D133A-D135I double and D135I point mutations completely prevented the inhibition of TREK-2 by RR (ANOVA, Scheffe's post hoc test, $p<10^{-5}$). The effect of the other mutations was not significant. (The numbers in the columns indicate the number of the measured oocytes.) **D.** The two subunits of TREK-2 dimer were expressed as a tandem construct (consisting of a single polypeptide chain), as indicated in the scheme illustrating transmembrane topology. Mutation of D135 in the upstream (*D135I/wt*, *blue*) or downstream (*wt/D135I*, *red*,) TREK-2 coding sequence reduced the inhibition by RR compared to the

construct composed of the wild type sequences (*wt/wt*, *green,* $p<0.001$). **E.** Normalized currents of wild type (*wt*), A108D-I110D double and I110D point mutant TREK-1 in the presence of RR (10 μM).

Fig. 4. Inhibition of TRAAK by different commercial preparations of ruthenium red.

A. Normalized currents of human and mouse TRAAK are plotted in the presence of different concentrations of RR purchased from Sigma in 2013. **B.** Similar measurement with an old RR preparation (Sigma 1996). Note the strong inhibition developing with slow kinetics. **C.** Dose-response relationships of TRAAK current (human (*hTRAAK*, *blue symbols*) or mouse (*mTRAAK*, *red symbols*)) and ruthenium red concentration (RR_{1996} or RR_{2013}, as indicated on the *right*) was calculated from the measurements in panel A and B, and fitted with the modified Hill equation (see *Methods*).

Fig. 5. Ruthenium violet inhibits TRAAK more potently than ruthenium red.

A. Absorption spectra of equal mass (w/v) concentration of ruthenium red purchased from Sigma in 1996 (RR_{1996}) or in 2013 (RR_{2013}), and our purified ruthenium violet preparation (RV). **B.** Dose-response relationship of mouse TRAAK current and $RR_{(2013)}$ or RV. **C.** Sensitivity of different K2P channels (as indicated *below* the *column graph*) to RV (1 μM) was measured. TASK-3, TREK-2 and mouse TRAAK were strongly inhibited. The D135I mutation of TREK-2 (*D135I* column) completely eliminated the sensitivity to RV.

Fig. 6. RR-sensitive background potassium current in DRG neurons

A. Representative current-voltage (I-V) relationships from a mouse DRG neuron. Currents were

measured in 2 mM (*black curve*) or 30 mM extracellular [K^+] in the absence (*blue*) or presence (*magenta*) of RR (10 μM) using a voltage protocol consisting of a step to -100 mV for 200 ms from a holding potential of -80 mV, followed by a 600 ms ramp to +60 mV. The I-V relationships were plotted from the ramp data. **B.** The difference current inhibited by RR in the presence of 30 mM [K^+] is calculated from the data shown in panel A (by subtracting the *magenta* curve from the *blue* one). **C.** Currents at -100 mV of the same DRG neuron as in panel A were plotted as the function of time. The currents measured during the voltage step to -100 mV are shown in the *inset*. **D.** Correlation between the K^+ current amplitude and the RR-sensitivity for 20 DRG neurons. The regression line (*red solid*) and 95 % confidence band (*red dotted curves*) of Pearson's correlation analysis are indicated. All DRG measurements were performed at 37 °C.

Fig. 7. Aspartate 135 residues are positioned in the extracellular ion pathway (EIP) above the selectivity filter.

The EIP tunnel is filled with a series of *blue* spheres in this schematic representation of human TREK-2 crystal structure (PDB ID: 4BW5, unpublished result of Pike ACW, et al.). K^+ ions in the vertical channel pore are illustrated with four solid (*tan*) spheres below the EIP. Aspartate 135 (D135) residues (*yellow* ball and stick representation, with *red* oxygen and *blue* nitrogen atoms) are located on the ceiling of the EIP above the selectivity filter. The two subunits are drawn as *red* and *green* ribbons. The view is not exactly perpendicular to the direction of the EIP, but the structure is slightly rotated around the vertical axis, in order to avoid the overlap of the D135 residues of the two subunits. The NSSN and NSSNNS sequences of the subunits, respectively, are not resolved by the crystal structure, however, this does not affect the EIP. The graphics were produced with MolAxis (Yaffe *et al.*, 2008) and VMD (Humphrey *et al.*, 1996) software.

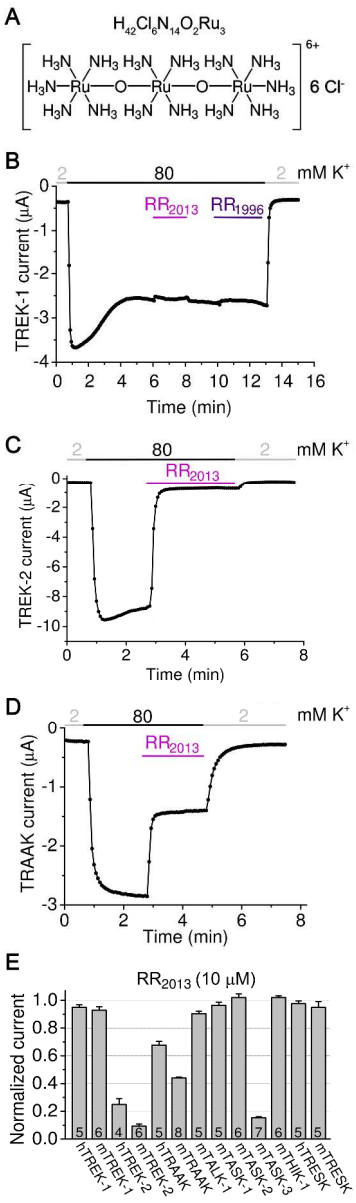

Fig. 1.
261x868mm (600 x 600 DPI)

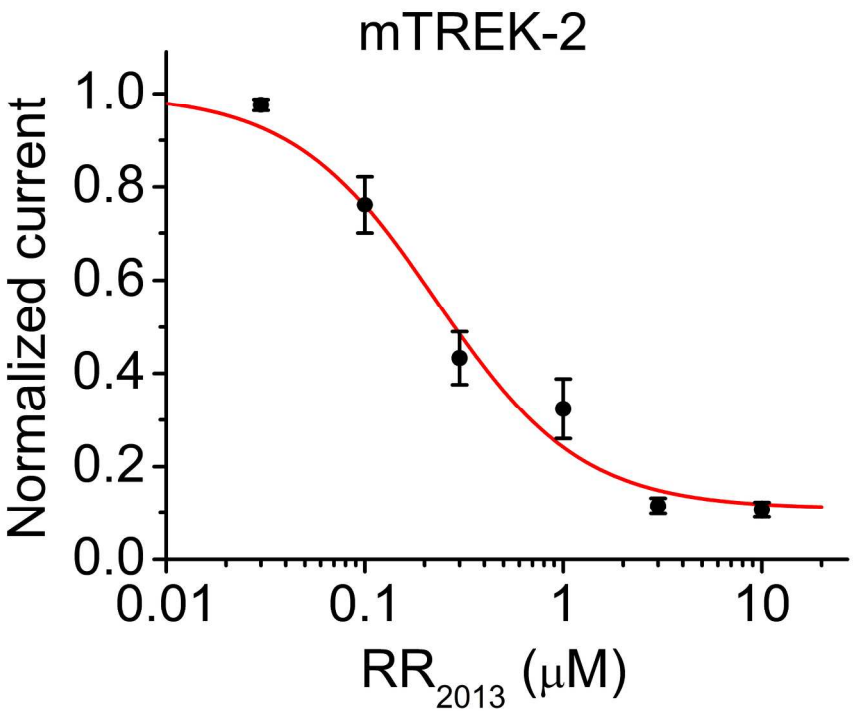

Fig. 2.
210x148mm (300 x 300 DPI)

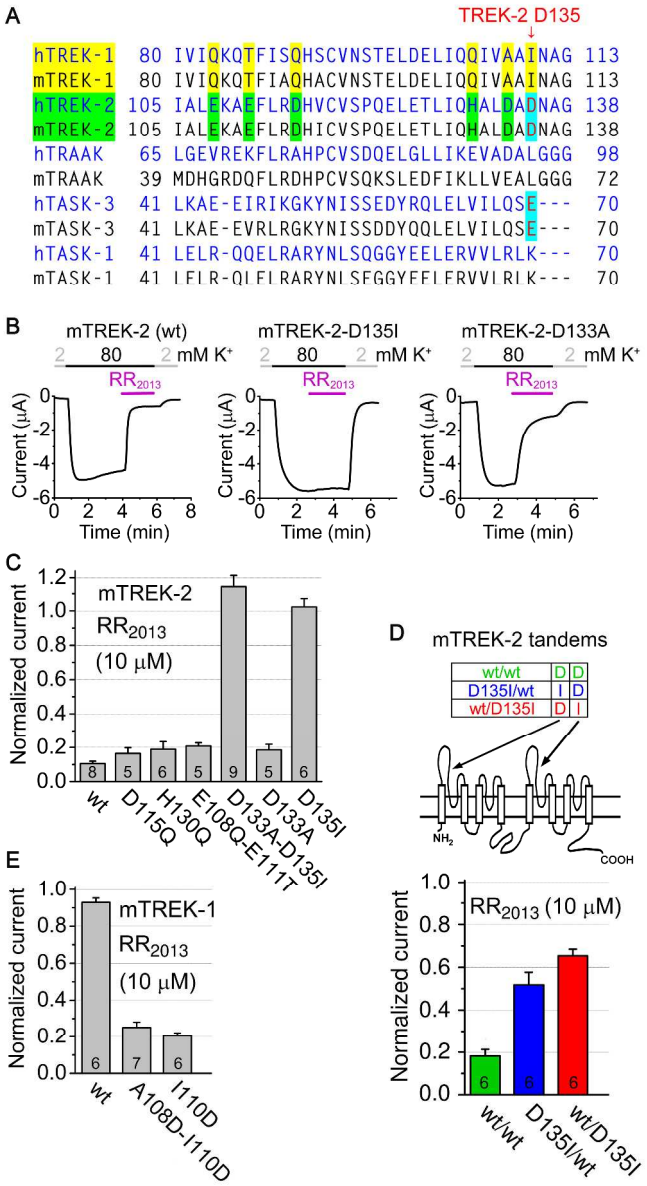

Fig. 3.
327x596mm (300 x 300 DPI)

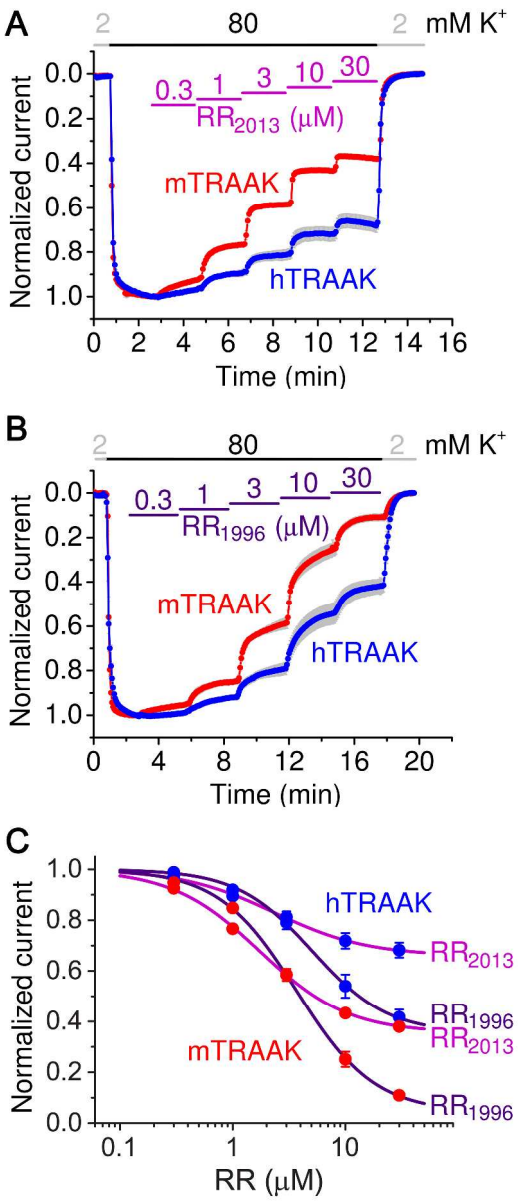

Fig. 4.
171x395mm (600 x 600 DPI)

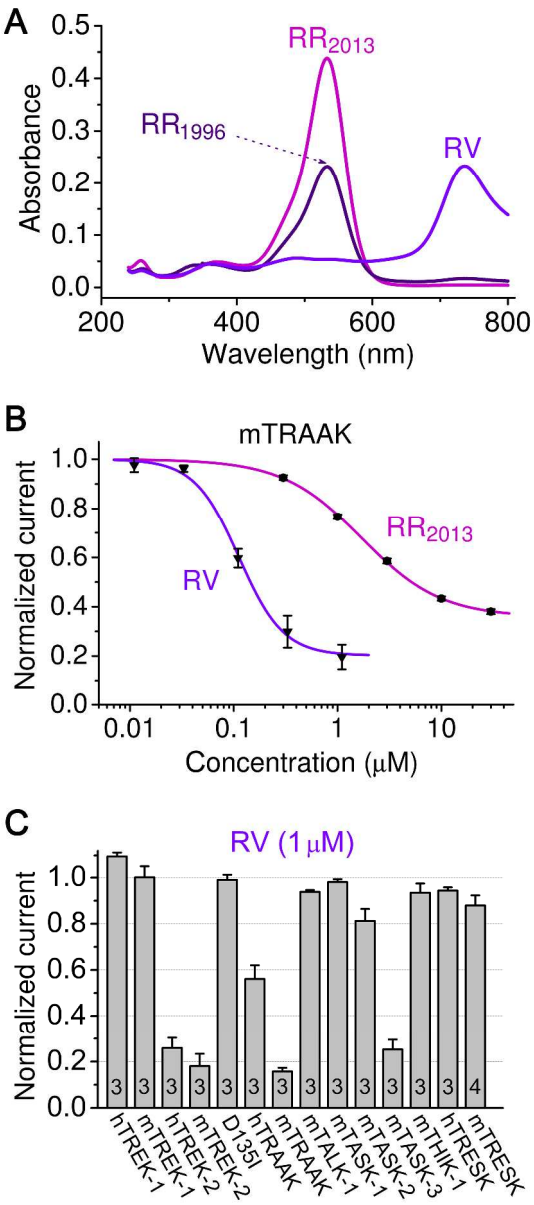

Fig. 5.
332x726mm (600 x 600 DPI)

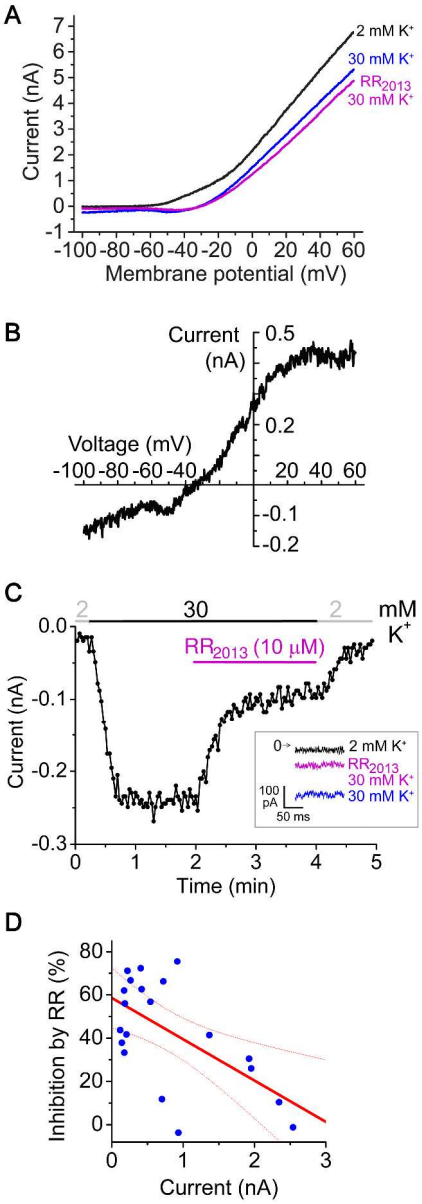

Fig. 6.
157x445mm (600 x 600 DPI)

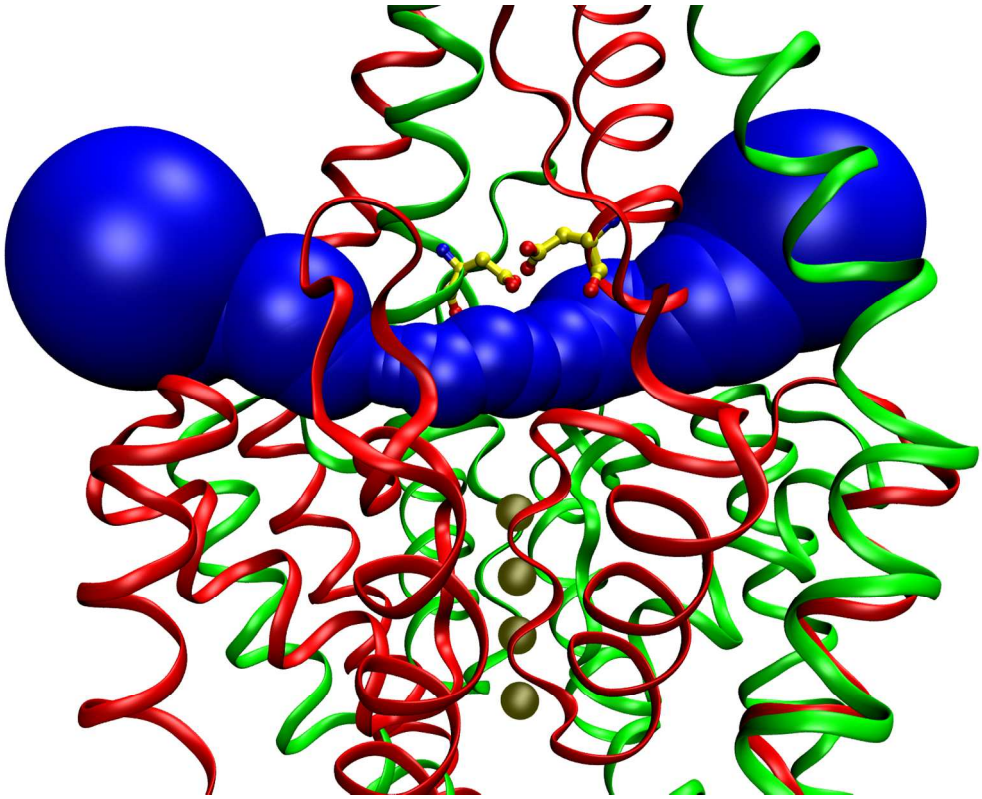

Fig. 7.
134x106mm (300 x 300 DPI)

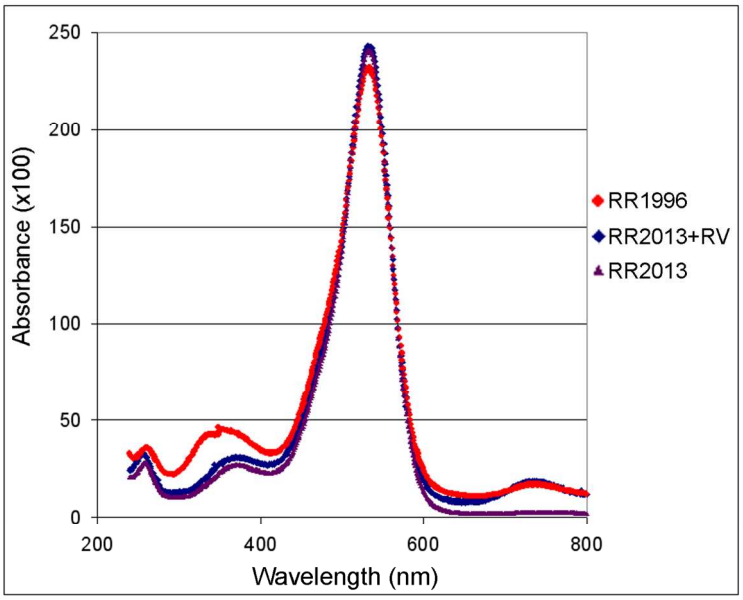

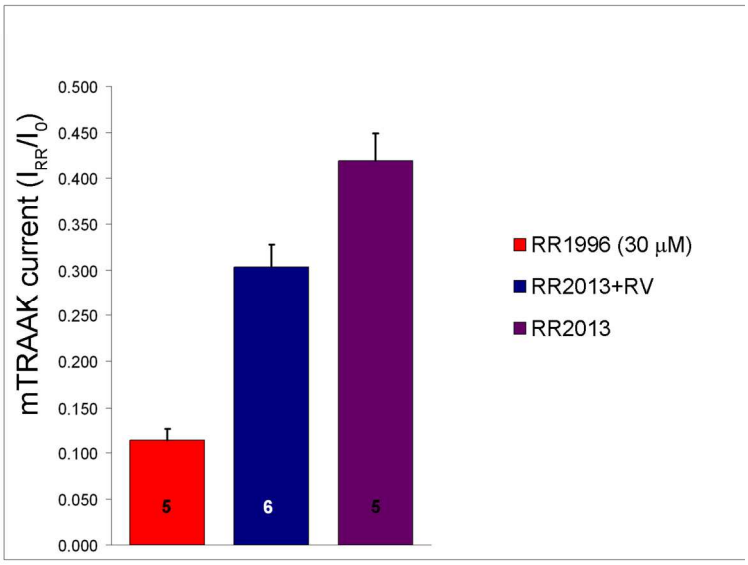

Supplementary Material
159x257mm (300 x 300 DPI)